https://doi.org/10.1016/j.ceramint.2017.11.198

Low-temperature-sintered $Bi_{0.5}Na_{0.5}TiO_3$-Based Lead-Free Ferroelectric Ceramics with Good Piezoelectric Properties

Tat-Hang Chung, Hailing Sun, Rui Wen and K.W. Kwok*,

Department of Applied Physics

The Hong Kong Polytechnic University, Kowloon, Hong Kong, China

Abstract

Li_2CO_3 has been used as a sintering aid for fabricating lead-free ferroelectric ceramic $0.93(Bi_{0.5}Na_{0.5}TiO_3)$-$0.07BaTiO_3$. A small amount (0.5 wt%) of it can effectively lower the sintering temperature of the ceramic from 1200°C to 980°C. Unlike other low temperature-sintered ferroelectric ceramics, the ceramic retains its good dielectric and piezoelectric properties, giving a high dielectric constant (1570), low dielectric loss (4.8%) and large piezoelectric coefficient (180 pC/N). The "depolarization" temperature is also increased to 100°C and the thermal stability of piezoelectricity is improved. Our results reveal that oxygen vacancies generated from the diffusion of the sintering aid into the lattices are crucial for realizing the low temperature sintering. Owing to the low sintering temperature and good dielectric and piezoelectric properties, the ceramics, especially of multilayered structure, should have great potential for practical applications.

Keywords: Low-temperature sintering; piezoelectric properties; BNTBT

* Corresponding author. Tel.: +852 27665667; fax: +852 23337629.

E-mail address: apkwkwok@polyu.edu.hk (K.W. Kwok)

1. Introduction

For the increasing environmental concern of lead-pollution, a large number of lead-free piezoelectric ceramics have been developed and studied extensively in recent years [1,2]. $Bi_{0.5}Na_{0.5}TiO_3$ (BNT) is one of the most promising candidates. It has a rhombohedral perovskite structure, with Bi^{3+} and Na^+ located at the A-sites of the ABO_3 structure. Although it has a large remanent polarization (P_r = 38 μC/cm^2), its high coercive field (E_c = 7.3 kV/mm) makes the poling difficult, and thus leading to weakened piezoelectric properties [3]. A number of works have been carried out for enhancing its piezoelectric properties. These include the formation of solid solutions with other ferroelectrics or non-ferroelectrics, e.g., BNT-$BaTiO_3$ (BNT-BT) [3-5], BNT-$Bi_{0.5}K_{0.5}TiO_3$ [6,7] and BNT-$BaTiO_3$-$KNbO_3$ [8]; and the doping of metal oxides, e.g., $(Bi_{0.5}Na_{0.5})_{1-1.5x}Bi_xTiO_3$ [9] and $Bi_{0.5}(Na_{1-x-y}K_xLi_y)_{0.5}TiO_3$ [10]. Among them, BNT-BT exhibits a high piezoelectric coefficient (d_{33}) and large electromechanical coupling coefficient (k_p) near the morphotropic phase boundary (MPB), i.e., 6-7 molar % of BT [4,5]. Similar to other ferroelectric ceramics, highly densified BNT-BT ceramics can normally be obtained at high sintering temperatures, typically above 1200°C. Although multilayered BNT-BT ceramics with Ag/Pd 70/30 inner electrodes have been fabricated at 1100-1140°C [11,12], the high sintering temperature will induce volatilization losses of Bi and Na and thus degradation of piezoelectric properties [13,14]. As a large displacement can be produced by a relatively low driving voltage that is essential for practical applications, multilayered ferroelectric ceramics have been widely used in actuator applications, especially for ultra-small scale precision motion devices and autofocus mechanism kits in phone and digital cameras.

Co-firing with inner electrodes is commonly employed in industries to fabricate multilayered ceramics for saving production time and cost as well as achieving better

adhesion and properties. In order to use relatively inexpensive inner electrodes such as Ag/Pd and prevent diffusions across the interfaces, low co-firing (or sintering) temperatures, e.g., below 1000°C, are commonly preferred, which are also crucial for ceramics containing volatile elements such as BNT-BT. Liquid-phase sintering technique, which is basically ascribed to the low melting temperature or eutectic points of sintering aids, is the common industrial approach for lowering the sintering temperature. A number of sintering aids, such as V_2O_5 [15], $BiFeO_3$+$Ba(Cu_{0.5}W_{0.5})O_3$ [16], Li_2CO_3-Bi_2O_3-$CdCO_3$ [17], $LiBiO_2$ [18] and Li_2CO_3 [19-21] have been shown effective in lowering the sintering temperature of various piezoelectric ceramics to below 1000°C. In general, the liquid formed in the early stage of sintering can wet the solid grains, increase the mass transport rate and then promote the grain coarsening and densification of the ceramics [22]. However, the liquid will form a secondary phase and generally degrade the electrical properties of the ceramics.

Valant et al. have shown that Li_2O can lower the sintering temperature of BT and $(Ba,Sr)TiO_3$ ceramics by more than 400°C, from ~1275 to 820°C and 1300 to 880°C, respectively [23]. A pre-reaction between Li_2O and BT at 600°C is required to form intermediate phases $BaCO_3$ and Li_2TiO_3 for achieving the low-temperature sintering. During sintering, one of the intermediate phases $BaCO_3$ “melts” at low temperature (811°C) and reacts with the other to release Li_2O, which then incorporates in BT and produces oxygen vacancies. Although the oxygen vacancies pay an important role in increasing the lattice-diffusion coefficient, the authors have suggested that the intermediate liquid phase $BaCO_3$ is essential as it can accelerate the mass-transport processes. Similar to other liquid-phase sintered ceramics, secondary phases (Li_2TiO_3 and Ba_2TiO_4) are formed, which may affect the dielectric and piezoelectric properties. However, the authors have not provided further discussions. Moreover, it has been

shown that $BaCO_3$ will not melt but just transform from an orthorhombic α phase to a trigonal β phase at 811°C [24], which makes the importance of the "intermediate liquid phase" become disputable. Binhayeeniyi et al. have lowered the sintering temperature of $Ba(Zr_{0.05}Ti_{0.95})O_3$ to 900°C using 1.5 wt% Li_2O [25]. The ceramic possesses a dense structure (with a density > 90% of theoretical density) and good piezoelectric property (with a d_{33} remained at 120 pC/N). A sol-gel route has been adopted in the study. As compared with the solid-state reaction method, the route itself can reduce the sintering temperature of un-doped ceramics from 1500°C to 1250°C. Recently, it has been shown that the sintering temperature of $Ba_{0.85}Ca_{0.15}Ti_{0.9}Zr_{0.1}O_3$ ceramics can be lowered from 1540°C to 1400°C after the doping of 0.3 wt% Li_2CO_3, while their piezoelectric coefficient is decreased by ~20%, from 650 to 512 pC/N [26]. Apparently, the sintering temperature (1400°C) is too high for multilayered ceramic applications in spite of the good piezoelectric properties. In this work, the sintering aid Li_2CO_3 will be used to lower the sintering temperature of $0.93(Bi_{0.5}Na_{0.5}TiO_3)$-$0.07BaTiO_3$ (BNTBT) ceramics, and its effects on the dielectric and piezoelectric properties will be studied. It will also be used to prepare $Bi_{0.485}Na_{0.485}Bi_{0.02}TiO_3$ (BNBiT) and $0.94K_{0.5}Na_{0.5}NbO_3$-$0.06BaTiO_3$ (KNNBT) ceramics for exploring the mechanism of lower-temperature sintering.

2. Experimental Procedure

BNTBT + x wt% Li_2CO_3 (BNTBT-Li-x) ceramics were prepared by a conventional ceramic fabrication technique using analytical-grade carbonate or metal oxide powders: Na_2CO_3 (99.5%), Bi_2O_3 (99.9%), TiO_2 (99.9%), $BaCO_3$(99.5%) and Li_2CO_3 (99%). The powders in the stoichiometric ratio of BNTBT were mixed thoroughly in ethanol using zirconia balls for 8 h, and then dried and calcined at 850°C for 2 h. After the calcination,

Li_2CO_3 powders were added. The mixture was then ball-milled again for 8 h, mixed thoroughly with a poly(vinyl alcohol) binder solution and then uniaxially pressed into disk samples with a diameter of 12 mm. The disk samples were finally sintered at 900 - 1080°C for 2 - 8 h in air. KNNBT and BNBiT ceramics added with 1 wt% Li_2CO_3 were also prepared following similar procedures.

The crystallite structures of the samples were examined using X-ray diffraction (XRD) analysis with CuK_α radiation (SmartLab; Rigaku, Tokyo, Japan). The microstructures were observed using a field-emission scanning electron microscope (FESEM) (JSM-6490; JEOL, Tokyo, Japan). The bulk density ρ was measured by the Archimedes method. The dielectric constant ε and dielectric loss tan δ were measured as functions of temperature using an impedance analyzer (HP 4194A, Agilent Technologies Inc., Palo Alto, CA). The piezoelectric coefficient d_{33} was measured at 50 Hz using a piezo-d_{33} meter (ZJ-3A, Institute of Acoustics, Chinese Academy of Sciences, Beijing, China). Before the dielectric and piezoelectric properties measurements, the ceramic samples were first coated with fired-on silver electrodes and then poled under a dc field of 5 kV/mm at 60°C in a silicone oil bath for 30 min.

3. Results and Discussion

Variations of the observed ρ and d_{33} for the BNTBT-Li-x ceramics sintered at different temperatures are shown in Fig. 1. The sintering time for the ceramic with x = 0 (i.e., without using Li_2CO_3) is 2 h, while 8 h has been used to sinter the other ceramics for compensating the (relatively) slower reactions resulted from the lower sintering temperatures. It can be seen that both the observed ρ and d_{33} generally increase and become saturated with increasing sintering temperature for all the ceramics. Similar to other BNT-based ceramics, the BNTBT-Li-0 ceramic achieves a dense structure (ρ >

95% of theoretical value) and good piezoelectric property (d_{33} = 190 pC/N) at a high sintering temperature of ~1200°C (Fig. 1a) [4,5]. After the addition of Li_2CO_3, the ceramics can be well densified at lower temperatures (Fig. 1b-d). As shown in Figs. 1b-c, the observed d_{33} for the ceramics with $x < 1$ saturates at a high value of ~180 pC/N, which is only about 5% lower than that of the high-temperature sintered BNTBT-Li-0 ceramic. On the other hand, although the BNTBT-Li-1 ceramic can be well densified to a high density, its d_{33} decreases considerably by ~30%, from 190 to 140 pC/N (Fig. 1d). Based on the results, the optimum sintering temperature for the ceramics, determined as the temperature at which the ceramic achieves the saturated density and piezoelectric property, have been obtained (Fig. 2). The saturated d_{33} for each ceramic is also shown in Fig. 2. It can be seen that a small amount of Li_2CO_3 (0.5 wt%) can lower the sintering temperature considerably from 1200 to 980°C. The piezoelectric property has not even been deteriorated significantly (only ~5%) after the low-temperature liquid-phase sintering.

Fig. 3 shows the variations of d_{33} with sintering time for the ceramics with $x = 0$, 0.5 and 1. All the ceramics are sintered at their optimum sintering temperatures (Fig. 2) for 2, 4 and 8 h. For the BNTBT-Li-0 ceramic, a longer sintering time leads to a reduction in d_{33}. This should be attributed to the non-stoichiometric composition resulted from the volatilization losses of Bi and Na during the high-temperature (1200°C) atmospheric sintering [11,12]. Apparently, a longer sintering time will result in more vaporization, and thus a larger degradation of piezoelectric property. On the other hand, a longer sintering time increases the observed d_{33} for the ceramics with x = 0.5 and 1. This should be partly attributed to the relatively slow mass transportation resulted from the low sintering temperatures. A longer time is thus required for completing the densification. The low sintering temperatures on the other hand would

reduce the volatilization losses of Bi and Na, and thus retaining the stoichiometric composition and good piezoelectric property. Based on these results, 2 and 8 h have been used as the optimum sintering time for fabricating the BNTBT-Li-0 and the other ceramics, respectively, in this work.

Fig. 4 shows the SEM micrographs of the BNTBT-Li-x ceramics sintered at their optimum conditions. In consistence with the density measurements, all the ceramics possess a dense structure and no abnormal grain growth is observed. It is interesting to note that after the addition of Li_2CO_3, the grains becomes larger at $x = 0.25$ (~ 1.8 μm) and smaller at $x \geq 0.5$ (~ 0.7 μm). The small grains should be caused by the low sintering temperatures (960°C) and the relatively slow mass transportation. As shown in Fig. 5, the observed ε_r (at 1 kHz) decreases from 1700 to 1520 as x increases from 0 to 1, while tan δ decreases slightly from 5.4 to 4.7%. The low dielectric loss also evidences the complete densification and dense structure of the ceramics.

Fig. 6 shows the XRD patterns of the BNTBT-Li-x ceramics sintered at their optimum conditions. All the ceramics possess a perovskite structure and, owing to the small amount or the resolution limit of the equipment, no secondary phases are observed. As evidenced by the shifting of the diffraction peaks (Fig. 6b), Li^+ should have diffused into the BNTBT lattices. All the ceramics exhibit a splitting of the (002)/(200) diffraction peaks, confirming that all of them reside near the MPB and contain both the rhombohedral and tetragonal phases. Owing to the similar ionic radii, Li^+ (1.41 Å, CN = 12) [27] should enter the A-sites of the BNTBT-Li-x ceramics (1.39 Å, average). The ionic radii of Bi^{3+}, Na^+ and Ba^{2+} for CN = 12 are 1.36 Å, 1.39 Å and 1.6 Å, respectively [28]. However, it has been shown that, regardless of the larger ionic difference (0.76 Å vs 0.61 Å, CN = 6) [29], Li^+ will substitute for the B-site Ti^{4+} of BNT-based ceramics when its concentration is high (e.g., > 0.75 mol%). It is thus

suggested that Li^+ has entered the A-site of the BNTBT-Li-x ceramics with $x < 0.5$ (i.e., ~ 1 mol%) and entered the B-site of the ceramics with $x \geq 0.5$. For all the ceramics, their lattices expand after the substitution with larger ions, and thus causing a shift of the diffraction peaks towards lower angles as shown in Fig. 6b. On the other hand, owing to the different valence states, oxygen vacancies are formed, in particular after the substitution of Ti^{4+} with Li^+, for maintaining the charge neutrality. As oxygen vacancies will cause the lattices to shrink [29], the lattice expansion of the ceramics with $x \geq 0.5$ arisen from the large ionic difference between Li^+ and Ti^{4+} is partially compensated, and thus engendering only a small shifting of the diffraction peaks as observed in Fig. 6b. The oxygen vacancies may also lead to a "hardening" effect causing the decreases in d_{33}, ε_r and tan δ as shown in Figs. 2 and 5 [30].

Although the ceramics contain (a small amount of) $BaTiO_3$, intermediate phases $BaCO_3$ and Li_2TiO_3 reported in the work of Valant et al. [23] should not have been formed (from the interaction of $BaTiO_3$ and Li_2CO_3) and exerted any effects on lowering the sintering temperature. It is suggested that the low-temperature sintering is attributed to the oxygen vacancies generated from the replacement of Ti^{4+} with Li^+, which increase the ionic lattice-diffusion coefficient and thus promote the densification at low temperatures [22,23,31]. On the other hand, as no intermediate phases (such as Ba_2TiO_4) are formed and left over, the good dielectric and piezoelectric properties of the BNTBT-Li-x ceramics (particularly those with $x < 1$) are retained.

To study further the conditions for low-temperature sintering, 1 wt% Li_2CO_3 has been used as a sintering aid to fabricate KNNBT (which contains similar Ba contents of BNTBT-Li-x) and BNBiT (which contains no Ba content) ceramics. The optimum sintering temperature and observed d_{33} and tan δ are summarized in Table 1. It can be seen that the sintering temperature of KNNBT is only lowered by ~90°C while the

observed d_{33} decreases significantly from ~90 to 55 pC/N [32]. Because of the similar ionic radii, Li^+ should has a larger preference of replacing the A-site ions (1.52 Å, average) than the B-site ions (0.61 Å, average). The ionic radius of K^+ is 1.64 Å (CN = 12) and that of Nb^{5+} is 0.64 Å (CN = 6) [28]. As a result, less oxygen vacancies would be generated (from the replacement of Ba^{2+} with Li^+), and thus the efficiency of low-temperature sintering is decreased. The decrease in d_{33} should be partly due to the deviation from the optimum MPB composition resulted from the incorporation of Li^+. On the other hand, the sintering temperature of BNBiT is lowered considerably by 170°C while its d_{33} remains almost unchanged at 90 pC/N (Table 1) [9]. Similar to BNTBT, owing to the high concentration (i.e., ~ 2 mol%), Li^+ should have entered the B-sites rather than the A-sites of BNBiT. As a result, oxygen vacancies are formed, the ionic lattice-diffusion coefficient is increased and the densification is promoted. Apparently, no intermediate phases relating to Ba^+ are formed and contributing to the low-temperature sintering.

Fig. 7 shows the temperature dependences of ε_r and tan δ for the poled BNTBT-Li-0 and BNTBT-Li-0.5 ceramics measured at 10 kHz, 100 kHz and 1000 kHz. Similar to the results published elsewhere [33,34], the BNTBT-Li-0 ceramic exhibits two distinctive anomalies, i.e., a frequency-dispersive shoulder at a lower temperature (~160°C) and a broad transition peak at a higher temperature (~300°C), confirming the relaxor characteristics. It has been shown that relaxor ferroelectrics contain largely polar nanoregions (PNRs), of which the thermal evolution gives rise to the dielectric anomalies [35]. Under a strong electric field, the randomly oriented PNRs will be aligned to form a ferroelectric state. Depending on the types of the relaxors, the aligned ferroelectric domains will retain (non-ergodic relaxors) or relax back to the randomly oriented PNRs (ergodic relaxors) upon the removal of the electric field [36]. Apparently,

the aligned ferroelectric domains (in poled non-ergodic relaxors) will be smashed and the randomly oriented PNRs will be restored upon heating. This will manifest as an abrupt change and/or a peak at T_d (depolarization temperature) in the temperature plots of ε_r and tan δ, respectively. It has been reported that BNTBT (i.e., BNTBT-Li-0) is a non-ergodic relaxor possessing a T_d of ~50°C [33]. However, the transition cannot be observed, because of the weakness, for the poled BNTBT-Li-0 ceramic in the present work. Nevertheless, as evidenced by its large d_{33} value (190 pC/N), it should be a non-ergodic relaxor at room temperature and its T_d should be around the reported value. For the BNTBT-Li-0.5 ceramic, the two anomalies merge into one, giving a single broad transition peak at ~250°C. Similar results have been reported for $0.95[0.94(Bi_{0.5}Na_{0.5-x}Li_x)TiO_3\text{-}0.06BaTiO_3]\text{-}0.05CaTiO_3$ ceramics attributing to the decrease in the composition ratio of the rhombohedral and tetragonal phases induced by the Li-substitution [37]. Our results can then substantiate the diffusion of Li^+ into the BNTBT lattices. On the other hand, a peak is barely observed at ~85°C (T_d) in the temperature plot of tan δ, indicating that the degree of ergoditcity is decreased and the aligned ferroelectric domains could retain at higher temperatures. Further investigation is needed to understand the mechanism of decreasing the degree of ergoditcity after the Li-addition.

The thermal stabilities of the BNTBT-Li-0 and BNTBT-Li-0.5 ceramics are thus compared by evaluating their retained d_{33} after thermal annealing (Fig. 8). The poled ceramics were annealed at various high temperatures for 0.5 h, and their d_{33} were re-measured at room temperature. As shown in Fig. 8, the observed d_{33} for the BNTBT-Li-0 ceramic starts to decrease as the annealing temperature increases from room temperature and shows a greater change at ~80°C. On the other hand, in consistent with the higher T_d (~85°C) as revealed in Fig. 7, the observed d_{33} for the BNTBT-Li-0.5

ceramic decreases only slightly at temperatures below 80°C, and starts to decrease rapidly at 100°C. These clearly confirm that the thermal stability of the ceramics has been improved after the diffusion of Li^+ into the lattices.

4. Conclusion

The effects of the sintering aid Li_2CO_3 on lowering the sintering temperature of lead-free ferroelectric ceramics BNTBT, KNNBT and BNBiT have been studied. Our results show that it can effectively lower the sintering temperature of BNTBT and BNBiT to below 1000°C, but not for KNNBT. For both the low temperature-sintered ceramics, their good piezoelectric properties are retained, which have seldom been reported for other low temperature-sintered ferroelectric ceramics. Our results also reveal that oxygen vacancies generated from the diffusion of the sintering into the lattices are not only essential for realizing low-temperature sintering but also beneficial for retaining the good electrical properties. Moreover, it can increase the "depolarization" temperature to 100°C and improve the thermal stability of BNTBT ceramics.

Acknowledgments

This work was supported by the Research Grants Council of the Hong Kong Special Administrative Region (Project No. PolyU 5170/13E).

REFERENCES

[1] T. Takenaka, H. Nagata, Current status and prospects of lead-free piezoelectric ceramics, J. Eur. Ceram. Soc. 25 (2005) 2693-2700.

[2] P.K. Panda, Review: environmental friendly lead-free piezoelectric materials, J. Mater. Sci. 44 (2009) 5049-5062.

[3] T. Takenaka, K. Maruyama, K. Sakata, $(Bi_{1/2}Na_{1/2})TiO_3$-$BaTiO_3$ system for lead-free piezoelectric ceramics, Japan. J. Appl. Phys. Part 1 30 (1991) 2236-2239.

[4] M. Chen, Q. Xu, B.H. Kim, B.K. Ahn, J.H. Ko, W.J. Kang, O.J. Nam, Structure and electrical properties of $(Na_{0.5}Bi_{0.5})_{1-x}Ba_xTiO_3$ piezoelectric ceramics, J. Eur. Ceram. Soc. 28 (2008) 843-849.

[5] C. Xu, D. Lin, K.W. Kwok, Structure, electrical properties and depolarization temperature of $(Bi_{0.5}Na_{0.5})TiO_3$-$BaTiO_3$ lead-free piezoelectric ceramics, Solid State Sci. 10 (2008) 934-940.

[6] A. Sasaki, T. Chiba, Y. Mamiya, E. Otsuki, Dielectric and piezoelectric properties of $(Bi_{0.5}Na_{0.5})TiO_3$-$(Bi_{0.5}K_{0.5})TiO_3$ systems, Jpn. J. Appl. Phys. 38 (1999) 5564-5567.

[7] K. Yoshii, Y. Hiruma, H. Nagata, T. Takenaka, Electrical properties and depolarization temperature of $(Bi_{1/2}Na_{1/2})TiO_3$-$(Bi_{1/2}K_{1/2})TiO_3$ lead-free piezoelectric ceramics, Jpn. J. Appl. Phys. 45 (2006) 4493-4496.

[8] J. Li, F. Wang, X. Qin, M. Xu, W. Shi, Large electrostrictive strain in lead-free $Bi_{0.5}Na_{0.5}TiO_3$-$BaTiO_3$-$KNbO_3$ ceramics, Appl. Phys. A 104 (2011) 117-122.

[9] X.X. Wang, K.W. Kwok, X.G. Tang, H.L.W. Chan, C.L. Choy, Electromechanical properties and dielectric behavior of $(Bi_{1/2}Na_{1/2})_{(1-1.5x)}Bi_xTiO_3$ lead-free piezoelectric ceramics, Solid State Commun. 129 (2004) 319-323.

[10] D. Lin, D. Xiao, J. Zhu, P. Yu, Piezoelectric and ferroelectric properties of

$Bi_{0.5}(Na_{1-x-y}K_xLi_y)_{0.5}TiO_3$ lead-free piezoelectric ceramics, Appl. Phys. Lett. 88 (2006) 062901.

[11] W. Krauss, D. Schütz, M. Naderer, D. Orosel, Klaus Reichmann, BNT-based multilayer device with large and temperature independent strain made by a water-based preparation process, J. Eur. Ceram. Soc. 31 (2011) 1857-1860.

[12] V.Q. Nguyen, J.K. Kang, H.S. Han, H.Y. Lee, S.J. Jeong, C.W. Ahn, I.W. Kim, J.S. Lee, Bi-based lead-free ceramic multilayer actuators using AgPd-$(Na_{0.51}K_{0.47}Li_{0.02})(Nb_{0.8}Ta_{0.2})O_3$ composite inner electrodes, Sens. Actuators, A 200 (2013) 107-113.

[13] Z.Z. Huang, H.L.W. Chan, K.W. Kwok, C.L. Choy, Preparation and electrical properties of $SrBi_2Ta_2O_9$ ceramics, J. Mater. Sci. 35 (2000) 1793-1797.

[14] K. Wang, J.F. Li, (K,Na)NbO_3-based lead-free piezoceramics: Phase transition, sintering and property enhancement, J. Adv. Ceram. 1 (2012) 24–37.

[15] D.E. Wittmer, R.C. Buchanan, Low-temperature densification of lead zirconate-titanate with vanadium pentoxide additive, J. Am. Ceram. Soc. 64 (1981) 485-490.

[16] S. Kaneko, D. Dong, K. Murakami, Effect of simultaneous addition of $BiFeO_3$ and $Ba(Cu_{0.5}W_{0.5})O_3$ on lowering of sintering temperature of $Pb(Zr,Ti)O_3$ ceramics, J. Am. Ceram. Soc. 1881 (1998) 1013-1018.

[17] W. Wang, K. Murakami, S. Kaneko, High-performance $PbZn_{1/3}Sb_{2/3}O_3$-$PbNi_{1/2}Te_{1/2}O_3$-$PbZrO_3$-$PbTiO_3$ ceramics sintered at a low temperature with the aid of complex additives Li_2CO_3-Bi_2O_3-$CdCO_3$, Jpn. J. Appl. Phys. 39 (2000) 5556-5559.

[18] R. Mazumder, A. Sen, 'Ultra'-low-temperature sintering of PZT: A synergy of nano-powder synthesis and addition of a sintering aid, J. Eur. Ceram. Soc. 28

(2008) 2731-2737.

[19] G.F. Fan, M.B. Shi, W.Z. Lu, Y.Q. Wang, F. Liang, Effects of Li_2CO_3 and Sm_2O_3 additives on low-temperature sintering and piezoelectric properties of PZN-PZT ceramics, J. Eur. Ceram. Soc. 34 (2014) 23-28.

[20] J. Yoo, C. Lee, Y. Jeong, K. Chung, D. Lee, D. Paik, Microstructural and piezoelectric properties of low temperature sintering PMN-PZT ceramics with the amount of Li_2CO_3 addition, Mater. Chem. Phys. 90 (2005) 386-390.

[21] Y.D. Hou, L.M. Chang, M.K. Zhu, X.M. Song, H. Yan, Effect of Li_2CO_3 addition on the dielectric and piezoelectric responses in the low-temperature sintered 0.5PZN–0.5PZT systems, J. Appl. Phys. 102 (2007) 084507.

[22] R.M. German, P. Suri, S.J. Park, Review: Liquid phase sintering, J. Mater. Sci. 44 (2009) 1-39.

[23] M. Valant, D. Suvorov, R.C. Pullar, K. Sarma, N.M. Alford, A mechanism for low-temperature sintering, J. Eur. Ceram. Soc. 26 (2006) 2777-2783.

[24] S.M. Antao, I. Hassan, $BaCO_3$: high-temperature crystal structures and the *Pmcn* $\rightarrow$ *R3m* phase transition at 811°C, Phys. Chem. Minerals 34 (2007) 573-580.

[25] N. Binhayeeniyi, P. Sukvisut, C. Thanachayanont, S. Muensit, Physical and electromechanical properties of barium zirconium titanate synthesized at low-sintering temperature, Mater. Lett. 64 (2010) 305-308.

[26] X. Chen, X. Ruan, K. Zhao, X. He, J. Zeng, Y. Li, L. Zheng, C.H. Park, G. Li, Low sintering temperature and high piezoelectric properties of Li-doped (Ba,Ca)(Ti,Zr)O_3 lead-free ceramics, J. Alloys Compd. 632 (2015) 103-109.

[27] C.W. Tai, S.H. Choy, H.L.W. Chan, Ferroelectric domain morphology evolution and octahedral tilting in lead-free $(Bi_{1/2}Na_{1/2})TiO_3$-$(Bi_{1/2}K_{1/2})TiO_3$-$(Bi_{1/2}Li_{1/2})TiO_3$-$BaTiO_3$ ceramics at different temperatures, J. Am. Ceram. Soc.

91 (2008) 3335-3341.

[28] R.D. Shannon, Revised effective ionic radii and systematic studies of interatomic distances in halides and chalcogenides, Acta Cryst. A32 (1976) 751-767.

[29] N. Lei, M. Zhu, P. Yang, L. Wang, L. Wang, Y. Hou, H. Yan, Effect of lattice occupation behavior of Li^+ cations on microstructure and electrical properties of $(Bi_{1/2}Na_{1/2})TiO_3$-based lead-free piezoceramics, J. Appl. Phys. 109 (2011) 054102.

[30] G. Li, L. Zheng, Q. Yin, Microstructure and ferroelectric properties of MnO_2-doped bismuth-layer $(Ca,Sr)Bi_4Ti_4O_{15}$ ceramics, J. Appl. Phys. 98 (2005) 064108.

[31] M.K. Zhu, L.Y. Liu, Y.D. Hou, H. Wang, H. Yan, Microstructure and electrical properties of MnO-Doped $(Na_{0.5}Bi_{0.5})_{0.92}Ba_{0.08}TiO_3$ lead-free piezoceramics, J. Am. Ceram. Soc. 90 (2007) 120-124.

[32] D.M. Lin, K.W. Kwok, H.L.W. Chan, Structure, dielectric, and piezoelectric properties of CuO-doped $K_{0.5}Na_{0.5}NbO_3$–$BaTiO_3$ lead-free ceramics, J. Appl. Phys. 102 (2007) 074113.

[33] C.M. Lau, X. Wu, K.W. Kwok, Photoluminescence, ferroelectric, dielectric and piezoelectric properties of Er-doped BNT–BT multifunctional ceramics, Appl Surf Sci. 336 (2015) 314-320.

[34] Y. Guo, Y. Liu, R.L. Withers, F. Brink, H. Chen, Large electric field-induced strain and antiferroelectric behavior in $(1- x)(Na_{0.5}Bi_{0.5})TiO_3$-$xBaTiO_3$ Ceramics, Chem Mater. 23 (2011) 219-228.

[35] W. Jo, S. Schaab, E. Sapper, L.A. Schmitt, H.J. Kleebe, A.J. Bell, J. Rödel, On the phase identity and its thermal evolution of lead free $(Bi_{1/2}Na_{1/2})TiO_3$-6 mol%$BaTiO_3$, J. Appl. Phys. 110 (2011) 074106.

[36] R. Dittmer, Lead-free piezoceramics - ergodic and nonergodic relaxor ferroelectrics based on bismuth sodium titanate, Technische Universität, Germany

[PhD Thesis] (2013).

[37] G. Viola, R. McKinnon, V. Koval, A. Adomkevicius, S. Dunn, H. Yan, Lithium-induced phase transitions in lead-free $Bi_{0.5}Na_{0.5}TiO_3$ based ceramics, J. Phys. Chem. C 118 (2014) 8564−8570.

Table 1 The optimum sintering, d_{33} and tan δ for the KNNBT and BNBiT ceramics added with 1 wt% Li_2CO_3

	Optimum Sintering Temperature (°C)	d_{33} (pC/N)	tan δ (%)
KNNBT[30]	1150	90	17
KNNBT + 1 wt% Li_2CO_3	1060	55	2.6
BNBiT[9]	1130	95	4.5
BNBiT + 1 wt% Li_2CO_3	960	90	3.7

FIGURE CAPTIONS

Fig. 1 Variations of ρ and d_{33} with sintering temperature for the BNTBT-Li-x ceramics.

Fig. 2 Optimum sintering temperature and d_{33} for the BNTBT-Li-x ceramics.

Fig. 3 Variations of d_{33} with sintering time for the BNTBT-L-x ceramics.

Fig. 4 SEM micrographs of the BNTBT-Li-x ceramics sintered at their optimum conditions.

Fig. 5 Variations of ε_r and tan δ (measured at 1 kHz) with x for the BNTBT-Li-x ceramics.

Fig. 6 XRD patterns of the BNTBT-Li-x ceramics.

Fig. 7 Temperature dependences of ε_r and tan δ for the BNTBT-Li-x ceramics with x = 0 (a) and 0.5 (b).

Fig. 8 Variations of retained d_{33} with annealing temperature for the poled BNTBT-Li-x ceramics with x = 0 and 0.5.

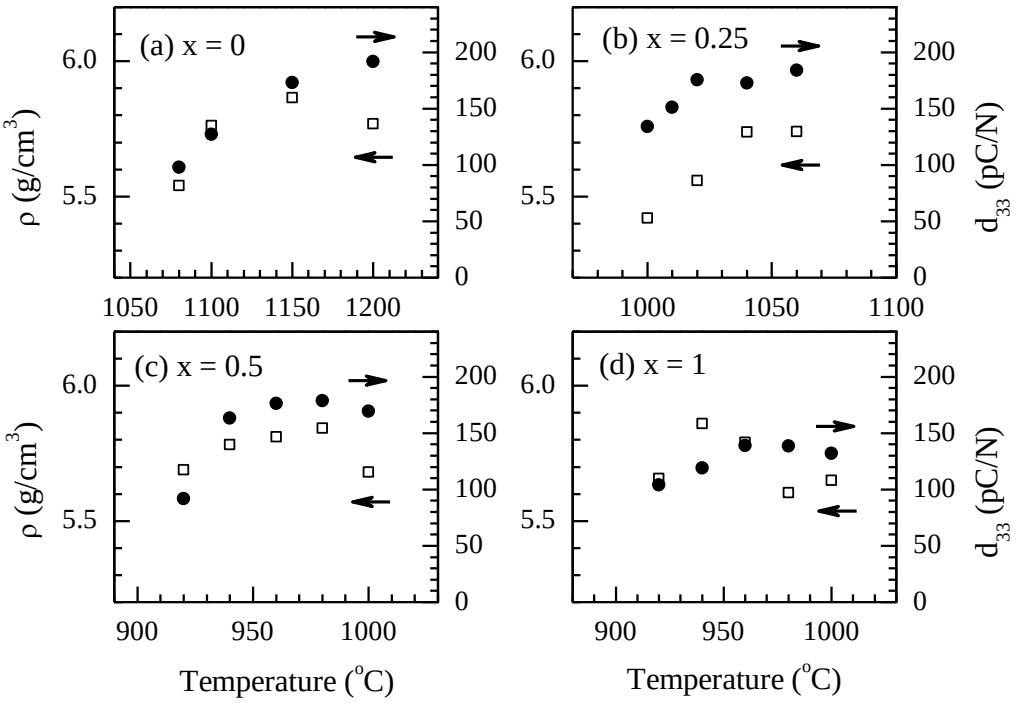

Fig. 1 Variations of ρ and d_{33} with sintering temperature for the BNTBT-Li-x ceramics.

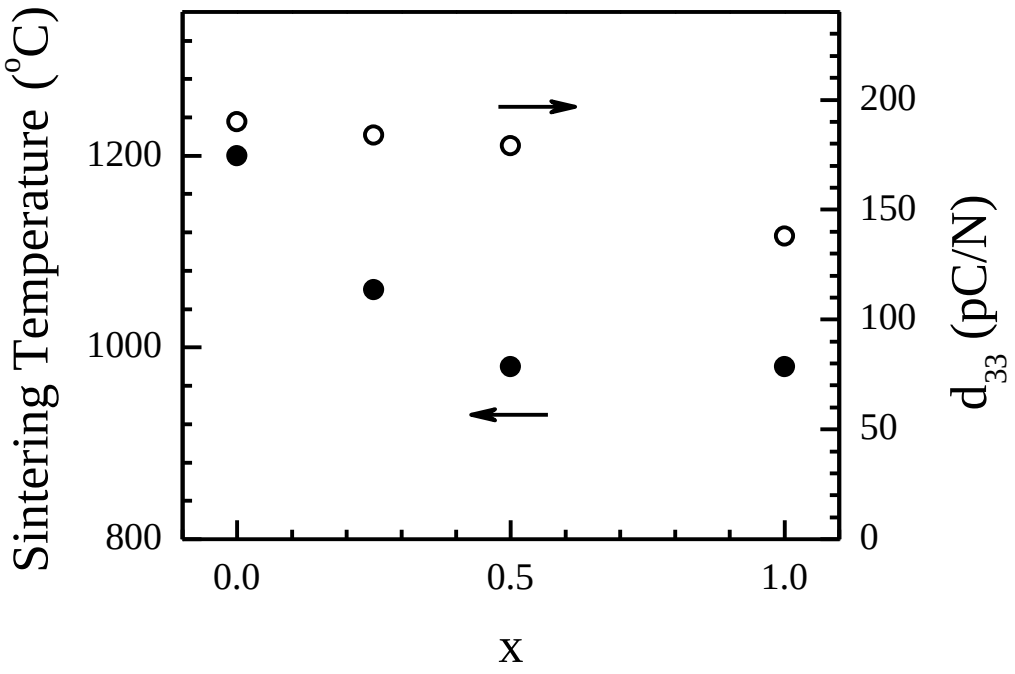

Fig. 2 Optimum sintering temperature and d_{33} for the BNTBT-Li-x ceramics.

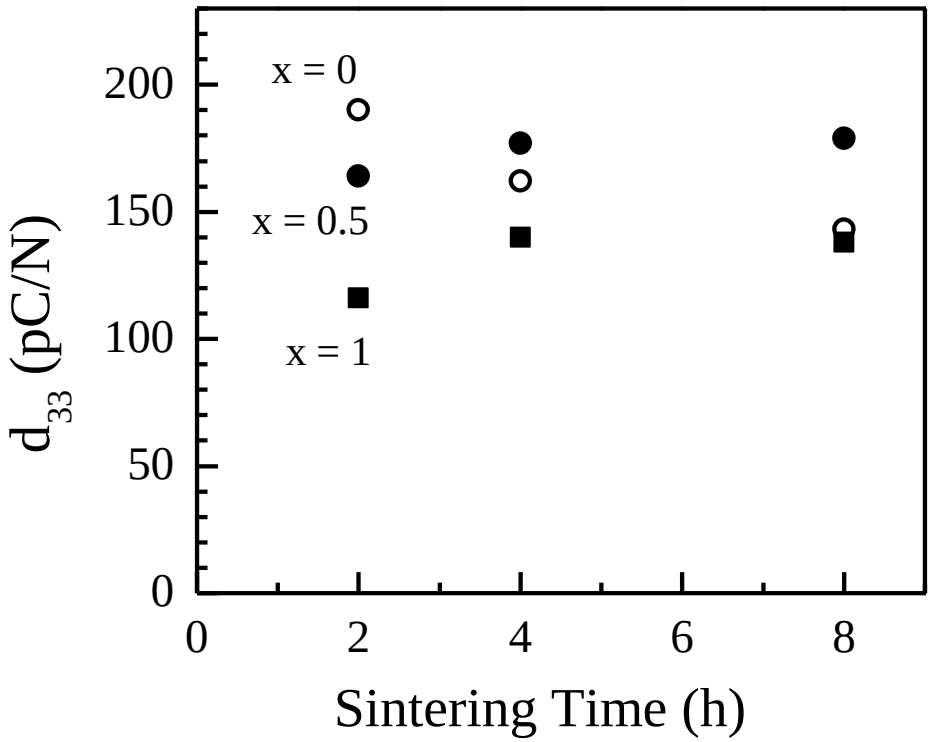

Fig. 3 Variations of d_{33} with sintering time for the BNTBT-L-x ceramics.

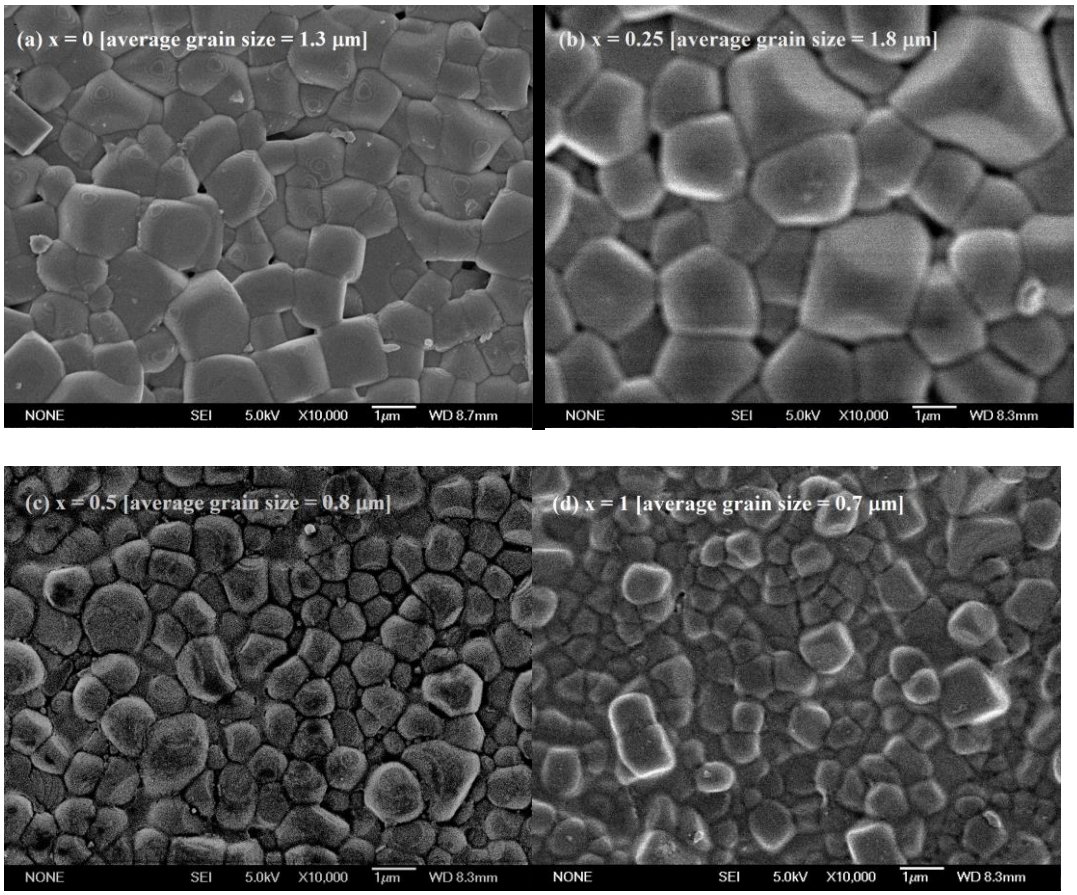

Fig. 4 SEM micrographs of the BNTBT-Li-x ceramics sintered at their optimum conditions.

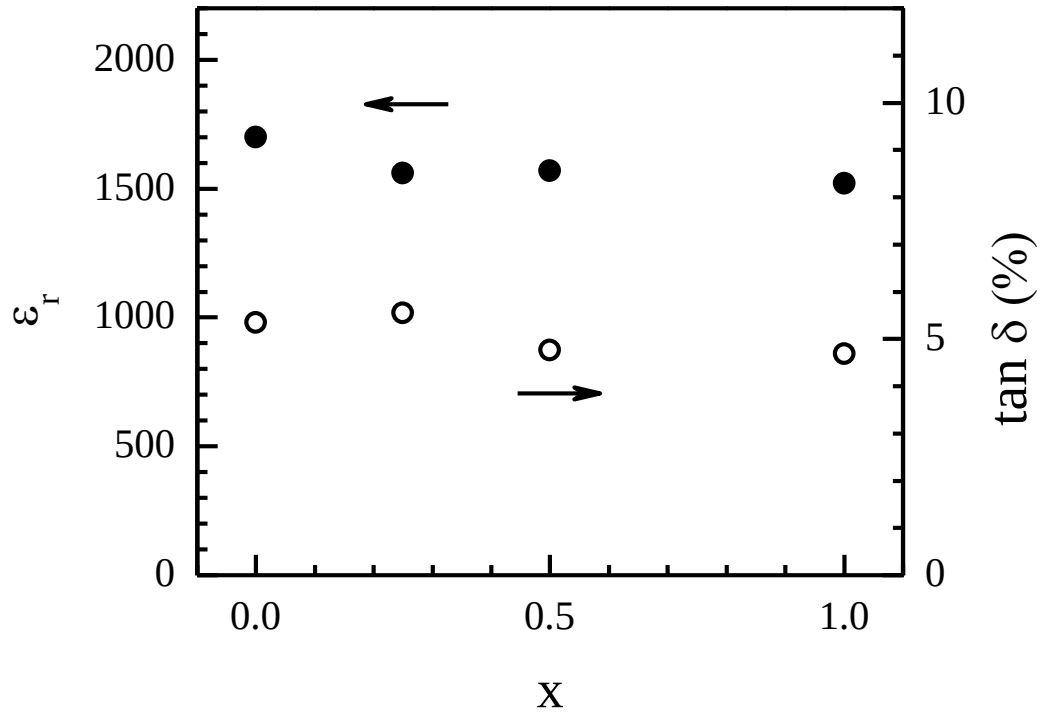

Fig. 5 Variations of ε_r and tan δ (measured at 1 kHz) with x for the BNTBT-Li-x ceramics.

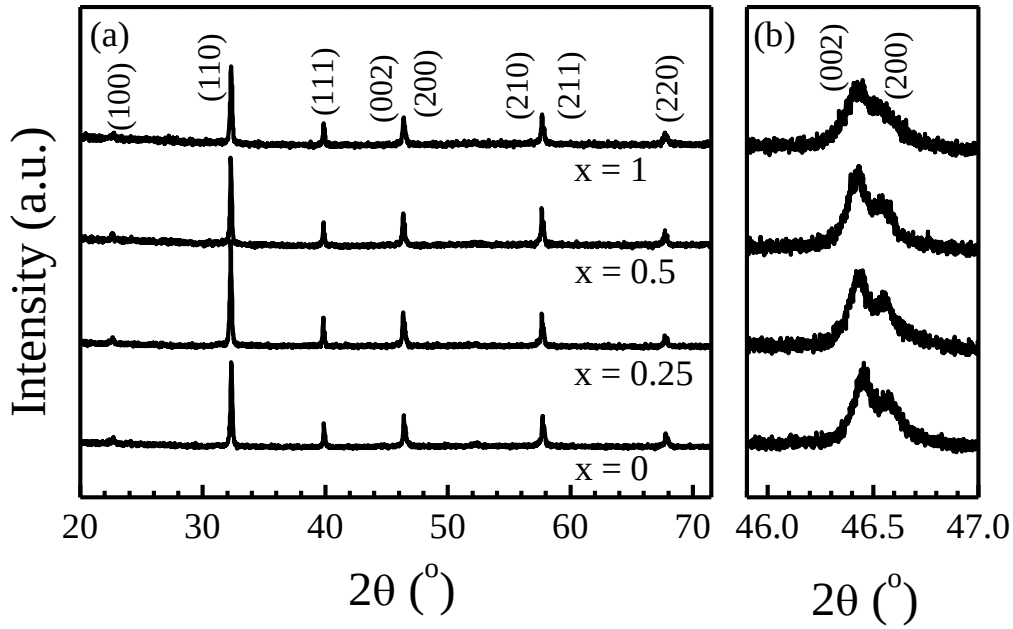

Fig. 6 XRD patterns of the BNTBT-Li-x ceramics.

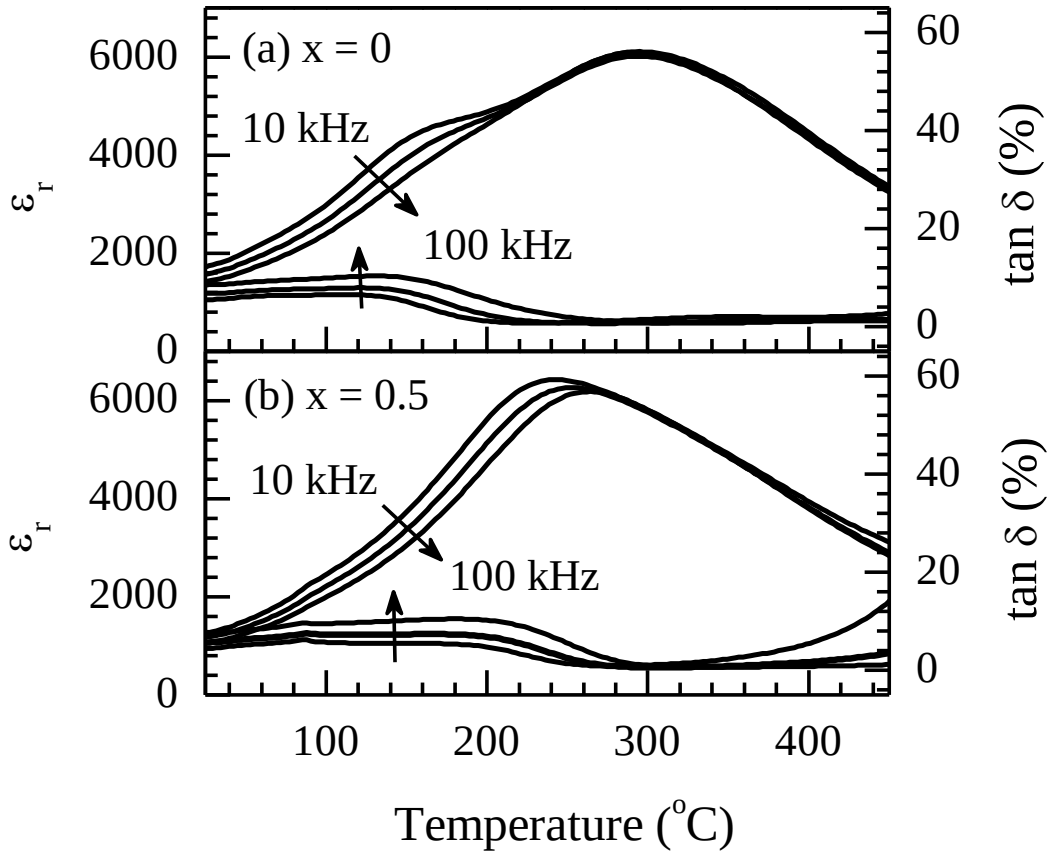

Fig. 7 Temperature dependences of ε_r and tan δ for the BNTBT-Li-x ceramics with x = 0 (a) and 0.5 (b).

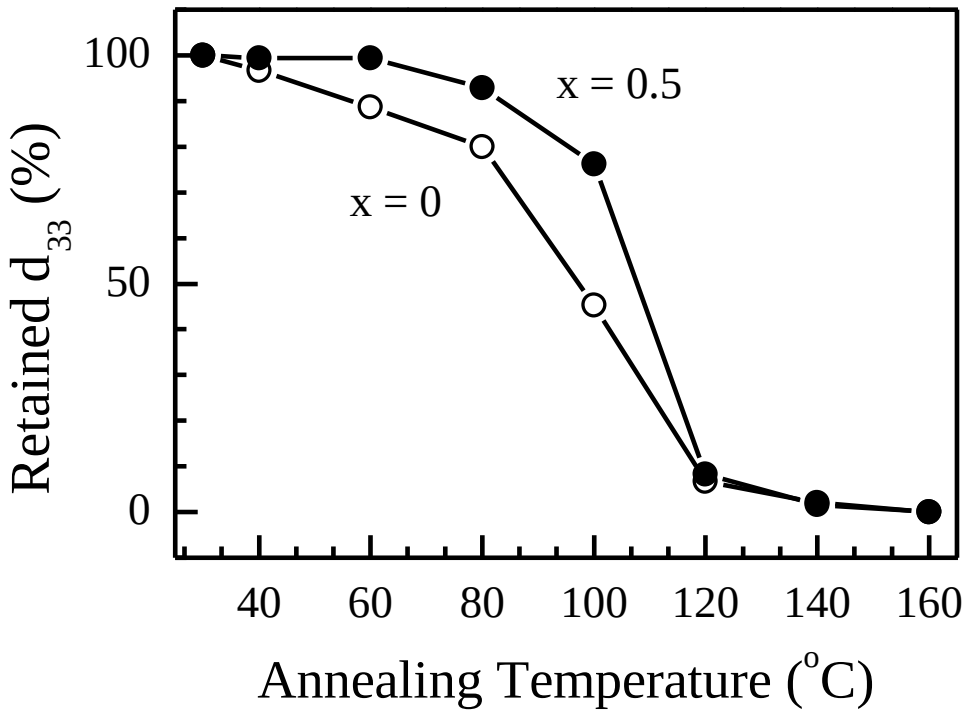

Fig. 8 Variations of retained d_{33} with annealing temperature for the poled BNTBT-Li-x ceramics with x = 0 and 0.5.